Int. J. Multiphase Flow Vol. 19, No. 6, pp. 987–997, 1993
Printed in Great Britain.

0301-9322/93 $6.00 + 0.00

PREDICTION OF LIQUID LEVEL DISTRIBUTION IN HORIZONTAL GAS–LIQUID STRATIFIED FLOWS WITH INTERFACIAL LEVEL GRADIENT

M. SADATOMI,[1] M. KAWAJI,[2]† C. M. LORENCEZ[2] and T. CHANG[2]

[1]Department of Mechanical Engineering, Kumamoto University, Kumamoto 860, Japan

[2]Department of Chemical Engineering and Applied Chemistry, University of Toronto, Toronto, Ontario, Canada M5S 1A4

(Received 6 November 1992; in revised form 11 August 1993)

Abstract—A one-dimensional momentum equation has been derived based on a two-fluid model and used to predict the axial distribution of liquid level or void fraction in steady, cocurrent, gas–liquid stratified flows in horizontal circular pipes and rectangular channels. The equation is carefully formulated to incorporate the effect of interfacial level gradient. Two different critical liquid levels are found from the momentum equation and are adopted as a boundary condition to calculate the liquid level or void fraction distribution upstream of the channel exit. The predicted void fraction distributions are compared with the experimental data obtained in a rectangular channel in this work and other data reported for large-diameter pipes. Good agreement is shown for air–kerosene, air–water and stream–water stratified flows with a smooth gas–liquid interface.

Key Words: multiphase flow, stratified flow, two-fluid model, interfacial level gradient, void fraction

1. INTRODUCTION

A stratified flow is a common two-phase flow pattern occurring in large-diameter horizontal pipes used in oil pipelines and in nuclear reactors during loss-of-coolant accidents. In this flow pattern, the gas and liquid phases are segregated due to gravity, and momentum is transferred between the phases at the gas–liquid interface due to shear.

Numerous studies have been conducted in the past on the stratified flow, but most are limited to flows in small-diameter pipes. Analytical models have also been developed for predicting the void fraction (or liquid holdup) and pressure drop in well-developed stratified flows, which do not display any significant interfacial level gradient (ILG) or the variation in the liquid level in the flow direction, dh_L/dx.

The stratified flows in large-diameter pipes, which are quite common in many industrial processes and plants, frequently show significant variations in the liquid level along the flow direction and somewhat peculiar holdup or void fraction behavior, especially at low mass velocities (Kawaji *et al.* 1987; Simpson *et al.* 1981). These stratified flows with nonzero ILG are not well understood at present and few studies are available in the literature.

Kawaji *et al.* (1987) conducted stratified flow experiments using steam and water at high pressures in a 180 mm i.d. pipe and measured the void fraction for two different exit conditions: the two-phase mixture flowing into a pool of liquid stored in a tank and the two-phase mixture freely-discharging into essentially an empty tank. Comparison of these data showed that the void fraction in the pipe is relatively uniform in the axial direction and independent of the exit condition if the mass velocity is $\gtrsim 400$ kg/m^{2}s, however, it is strongly influenced by the exit condition if the mass velocity is < 100 kg/m^{2}s. The physical reasons for these interesting results were not apparent at that time and an analytical model is needed to fully explain them.

Bishop & Deshpande (1986) pointed out that there are some stratified flow void fraction data, published in the past, that cannot be predicted by correlations derived for a well-developed stratified flow. They suggested incorporating an ILG term in an analytical model, but their model could not be used for calculation of the liquid level distribution, so they did not attempt such an

†To whom all correspondence should be addressed.

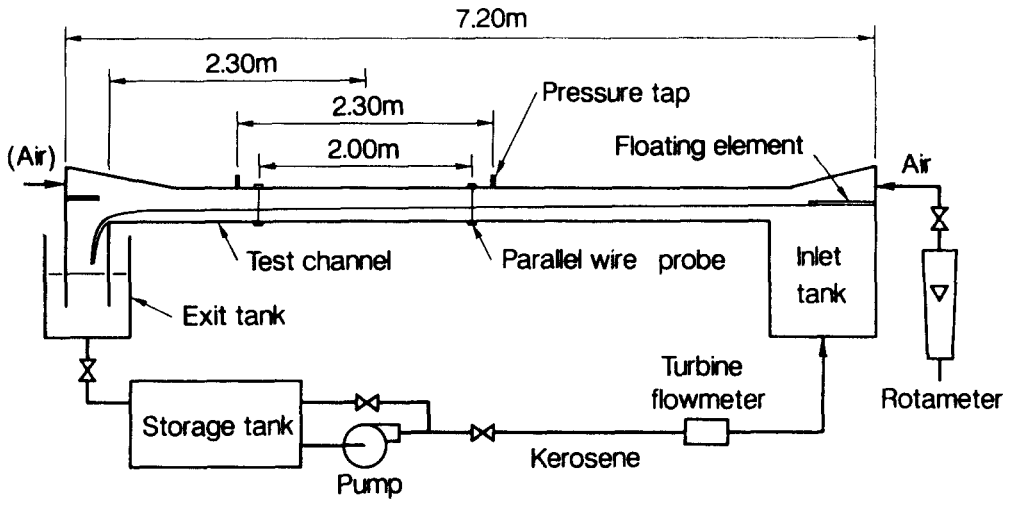

Figure 1. Two-phase test loop.

analysis. They further stated that although the pressure gradients in the liquid and gas are expected to be different from each other, their relationship is still unclear and should therefore be studied by measuring both gradients at the same time.

More recently, Koizumi *et al.* (1990) have conducted air–water two-phase flow experiments in a 210 mm i.d. horizontal pipe and obtained reliable void fraction data for stratified flows with ILGs. They have shown that these data can be predicted relatively well by an open-channel flow model involving only the liquid phase. The experiments and analysis were limited to the case of a free-discharge condition at the exit.

In this work, a one-dimensional two-fluid model is formulated based on a momentum balance for stratified flows with ILGs. The final equations derived are the same as those previously reported by Taitel & Dukler (1987); however, the derivation of the equations uses a different approach and considers the balance of all the forces in a comprehensive manner. Based on the equations derived, two different critical liquid levels are found to exist at the exit of the flow channel depending on the discharge condition, and they are used as the boundary condition for the two-fluid model to calculate the void fraction or liquid level distribution along the pipe axis. The model is thus applicable to both cases of free-discharge and discharge into a pool of liquid at the flow channel exit. The model is tested by predicting the void fraction data obtained in this work for a rectangular duct and other data obtained in circular pipes previously reported by Kawaji *et al.* (1987), Koizumi *et al.* (1990) and Simpson *et al.* (1981).

2. EXPERIMENTS

The experimental apparatus used in the present work is shown schematically in figure 1. The working fluids were air and kerosene (density, $\rho = 752\ \text{kg/m}^3$; dynamic viscosity, $\mu = 1.31 \times 10^{-3}$ Pa-s) at room temperature and atmospheric pressure. The test section was a horizontal, rectangular duct 50.8 mm high and 101.6 mm wide, and the inlet and outlet chambers were designed to handle both cocurrent and countercurrent stratified flows as previously described by Lorencez *et al.* (1991). A floating plate was used in the liquid inlet tank to minimize generation of interfacial waves. The gas and liquid flow rates were measured using a precalibrated rotameter (uncertainty 2%) and a turbine flow meter (uncertainty 1%).

The liquid level was measured using two pairs of parallel nichrome wires located at 1.3 and 3.3 m from the liquid inlet. The wires were 0.2 mm dia and 1.0 mm apart, and vertically set at the center of the channel cross section. Since kerosene's electrical conductivity is very low, a DC source could not be used as in previous studies by Brown *et al.* (1978) and Koskie *et al.* (1989). Instead, an AC source was used and the capacitance between the wires was measured to obtain the liquid level. The measurement system was carefully calibrated against the liquid levels measured with a needle

connected to a micrometer and inserted from the top of the channel. Penetration of the needle through the interface caused formation of a thin streak on the liquid surface and could easily be checked visually for a smooth interface. The uncertainty in the measured results were ± 0.1 mm for the liquid level and $\pm 0.2\%$ for the void fraction.

3. ANALYSIS

3.1. Physical model

The stratified flow being modeled and the symbols used in the model are shown in figure 2. The gas and liquid are assumed to flow in the same direction without any phase change in a circular, horizontal pipe and the interface between the two phases is assumed to be smooth but the liquid level can vary in the flow direction. Although the final equations developed here are the same as those reported earlier by Taitel & Dukler (1987), in deriving the momentum equation, we have paid particular attention to the relationship between the pressure gradients in the two phases, as suggested by Bishop & Deshpande (1986), and considered all the forces acting on the fluid boundaries in a comprehensive manner.

As shown in figure 2, if the liquid level is given by h_L, the centroid of the liquid cross section is located at kh_L below the interface, where k is given by the following equation:

$$k = [(\pi - \theta)\cos\theta + (\sin\theta) - \sin^3\theta/3]/[(1 + \cos\theta)(\pi - \theta + \sin\theta\cos\theta)]. \quad [1]$$

This centroid parameter varies with the liquid level, so if an ILG exists, the value of k will vary with the axial distance. Using the parameter, k, the average pressures in the gas and liquid phases are related as follows:

$$P_L = P_G + k\rho_L g h_L. \quad [2]$$

The pressures P_L and P_G are defined as the area-averaged pressures for the liquid and gas cross-sections, respectively.

Differentiation of [2] with respect to the axial coordinate yields

$$(dP_L/dx) = (dP_G/dx) + \rho_L g\, d(kh_L)/dx. \quad [3]$$

The cross-sectional areas, A_L and A_G, hydraulic diameters, D_L and D_G, wetted perimeters, l_{WL} and l_{WG}, and the interfacial area per unit axial length, l_i, can be represented as simple functions of the inner diameter, D, liquid level, h_L, and/or angle, θ, as given by Taitel & Dukler (1976a).

The shear stresses at the fluid–wall boundary, τ_{WL} and τ_{WG}, and at the interface, τ_i, are given by

$$\tau_{WL} = f_L \rho_L U_L^2/2 \quad [4]$$

and

$$\tau_{WG} = \tau_i = f_G \rho_G U_G^2/2. \quad [5]$$

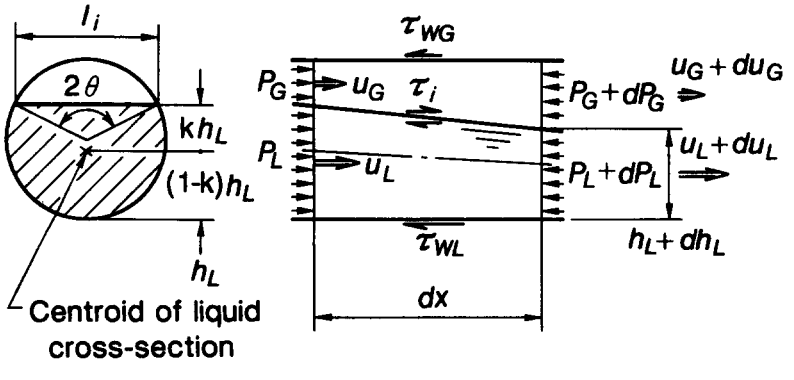

Figure 2. Flow geometry and symbols.

Here, U_L and U_G are the average velocities of the liquid and gas in cross-sectional areas A_L and A_G, respectively. For flows in large pipes, since the Reynolds numbers (as defined below) are usually greater than 2000 for both phases, the Blasius relation can be used for the friction factors, f_L and f_G, in [4] and [5]:

$$\mathrm{Re}_L = \rho_L U_L D_L/\mu_L; \quad \mathrm{Re}_G = \rho_G U_G D_G/\mu_G. \tag{6}$$

It is noted that although the cross sections of the flow areas occupied by both phases are noncircular, the difference between the laminar friction factor expressions for the present noncircular and circular cross sections is $<3\%$ (Shah & London 1978). Thus, for turbulent flow, the difference is expected to be even smaller and the Blasius relation should be applicable without any modification (Sadatomi *et al.* 1982).

3.2. Momentum equation

Based on a one-dimensional two-fluid model, the momentum equation for the liquid phase is given by

$$P_L A_L - (P_L + \mathrm{d}P_L)(A_L + \mathrm{d}A_L) - \tau_{WL} l_{WL} \mathrm{d}x + \tau_i l_i \mathrm{d}x + \rho_L U_L^2 A_L - \rho_L U_L A_L (U_L + \mathrm{d}U_L) + (P_G + \mathrm{d}P_G/2)\,\mathrm{d}A_L = 0. \tag{7}$$

The last term on the LHS of [7] is the x-component of the pressure force acting on the inclined interface from the gas side. By combining with the liquid continuity equation and neglecting the terms of small order, [7] becomes

$$-(\mathrm{d}P_L/\mathrm{d}x) - \tau_{WL} l_{WL}/A_L + \tau_i l_i/A_L - (k\rho_L g h_L - \rho_L U_L^2)(\mathrm{d}A_L/\mathrm{d}x)/A_L = 0. \tag{8}$$

In a similar manner, the following momentum equation is obtained for the gas phase, assuming constant density:

$$-(\mathrm{d}P_G/\mathrm{d}x) - \tau_{WG} l_{WG}/A_G - \tau_i l_i/A_G - \rho_G U_G^2 (\mathrm{d}A_L/\mathrm{d}x)/A_G = 0. \tag{9}$$

Combining [3], [8] and [9], we obtain the following momentum equation:

$$\tau_{WG} l_{WG}/A_G - \tau_{WL} l_{WL}/A_L + \tau_i l_i (1/A_G + 1/A_L) = \rho_L g [k h_L (\mathrm{d}A_L/\mathrm{d}x)/A_L + \mathrm{d}(k h_L)/\mathrm{d}x] - (\rho_G U_G^2/A_G + \rho_L U_L^2/A_L)(\mathrm{d}A_L/\mathrm{d}x). \tag{10}$$

The first term on the RHS can be written as follows:

$$\rho_L g [k h_L/A_L + \mathrm{d}(k h_L)/\mathrm{d}A_L](\mathrm{d}A_L/\mathrm{d}x) \tag{11}$$

and, furthermore, it can be readily shown that

$$k h_L/A_L + \mathrm{d}(k h_L)/\mathrm{d}A_L = 1/(D \sin\theta) = 1/l_i \tag{12}$$

and

$$\mathrm{d}A_L/\mathrm{d}x = l_i(\mathrm{d}h_L/\mathrm{d}x). \tag{13}$$

The momentum equation [10] can then be written as follows:

$$\tau_{WG} l_{WG}/A_G - \tau_{WL} l_{WL}/A_L + \tau_i l_i (1/A_G + 1/A_L) = [\rho_L g - l_i(\rho_G U_G^2/A_G + \rho_L U_L^2/A_L)](\mathrm{d}h_L/\mathrm{d}x). \tag{14}$$

Taitel & Dukler (1987) have proposed the same momentum equation as [14] for stratified flows with ILGs. Here, a different approach, based on comprehensive treatment of the liquid and gas pressure gradients, has been used to derive the momentum equation. It is also noteworthy that if the flow is well-developed and the ILG, $\mathrm{d}h_L/\mathrm{d}x$, is negligible, the RHS of [14] becomes zero and the momentum equation reduces to the form given by Taitel & Dukler (1976a) for a zero-ILG flow.

In order to show the importance of the terms on the RHS of [14], Koizumi *et al.*'s (1990) void fraction data were compared with [14]. Their experiments were performed at atmospheric pressure using air and water flowing in a 30.5 m long circular pipe with 210 mm i.d. From their void fraction data, obtained at 7.42 and 26.78 m downstream of the mixing section, the average void fraction and the ILG, $\mathrm{d}h_L/\mathrm{d}x$, were computed for several runs with a smooth interface.

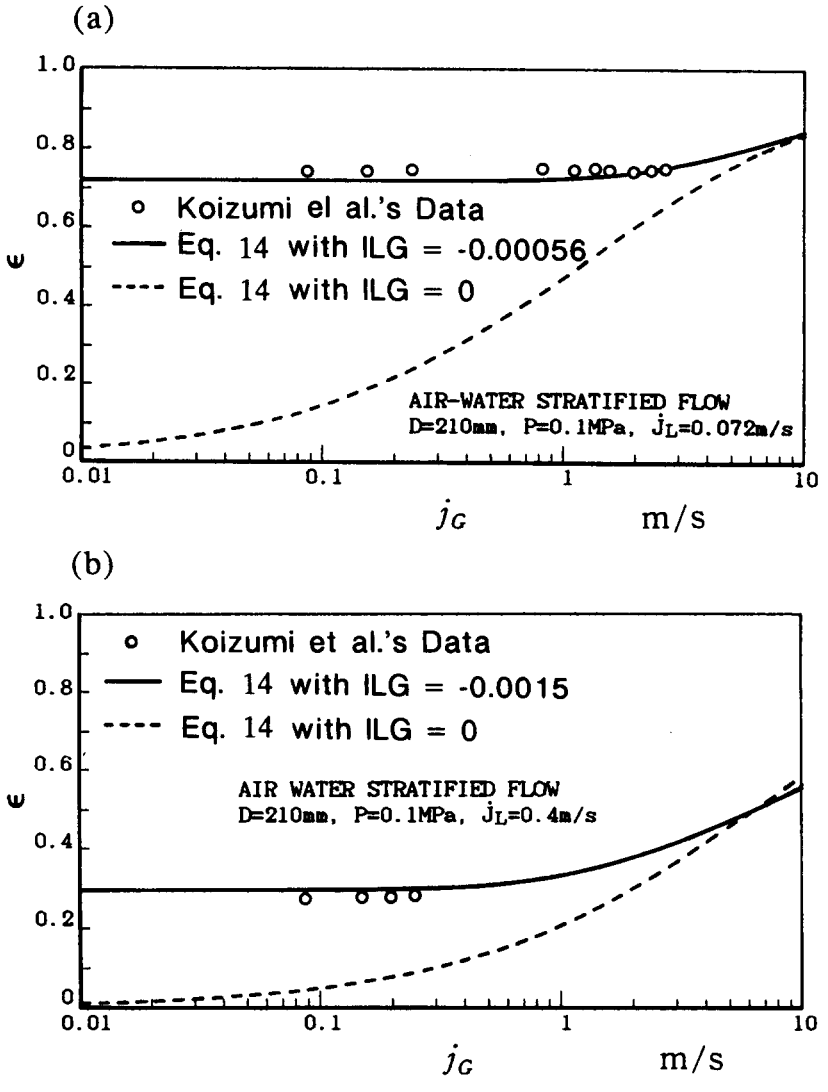

Figure 3. Comparison of momentum equation predictions with Koizumi *et al.*'s (1990) data.

Their data showed that the ILG was dependent principally on the superficial liquid velocity, j_L, and little influenced by the superficial gas velocity, j_G. Thus, the ILG value was assumed to be constant for a given liquid flow rate and using the ILG value, [14] was solved to obtain the average void fraction.

Comparison of the predicted and experimental void fraction values, ϵ, is shown in figures 3(a) and 3(b), corresponding to the smallest and the largest liquid flow rates in Koizumi *et al.*'s (1990) experiments, respectively. In both cases, the predictions of [14] with the measured values used for the ILG ($=dh_L/dx$) are indicated by solid curves and are seen to be in good agreement with the data. The predictions with zero-ILG, shown by broken lines in both cases, deviate away from the data as j_G is reduced. This shows the importance of incorporating the ILG term in the momentum equation, particularly at low liquid and gas flow rates. A method to predict the liquid level distribution and the ILG will be described in the following sections.

3.3. Critical liquid level

In an open-channel flow of a liquid, a critical liquid level is reached near the exit of the channel for a free-discharge condition and its value is determined by imposing the condition of an infinite level gradient (French 1985). It is reasonable to consider that a similar critical liquid level exists

in two-phase stratified flow (Taitel & Dukler 1987), and thus the momentum equation derived earlier is now examined to determine the critical liquid level in stratified flows.

The LHS of [14] is not equal to zero unless the flow is well-developed and the ILG, dh_L/dx, is zero. The critical level is obtained if the ILG is set to either positive or negative infinity, so that

$$\rho_L g - l_i(\rho_G U_G^2/A_G + \rho_L U_L^2/A_L) = 0. \quad [15]$$

The liquid level, h_L, that satisfies [15] is the critical level, however, this equation may or may not possess a solution depending on the gas and liquid flow rates, pipe diameter and fluid densities. For given fluid densities and pipe diameter, the combinations of gas and liquid velocities that yield a solution can be easily determined and a boundary of the solution domain can be drawn as a curve on a j_L vs j_G map.

For example, the boundaries of the solution domain for different pipe diameters from $D = 10$ to 200 mm are shown in figure 4(a) for an air–water system at atmospheric pressure and in figure 4(b) for a steam–water system at 7.45 MPa, corresponding to Kawaji *et al.*'s (1987) experiments. In the region above each curve, there is no solution for [15]. On the other hand, below the boundary curve there are two solutions corresponding to two critical liquid levels that can exist for different discharge conditions.

Since there is always a normal liquid level which is reached in a well-developed stratified flow with zero-ILG, we can state that in any stratified flow there are three possible liquid levels (two critical and one normal) in the velocity domain below the boundary curve and only one level (normal) above the curve. In the latter domain, the liquid's kinetic energy term, $\rho_L U_L^2/A_L$, becomes so large that [15] does not have a solution and only the normal liquid level can be considered as the limiting value.

The flow pattern transition boundary between the stratified and intermittent flows given by Taitel & Dukler's (1976b) equation,

$$U_G = (1 - h_L/D)[(\rho_L - \rho_G)gA_G/(\rho_G\, dA_L/dh_L)]^{1/2}, \quad [16]$$

is also shown in figure 4(a) by a broken line for an air–water flow in a 25 mm i.d. pipe. Below the broken line lies the stratified flow region and the present model is applicable only to this region. It should be noted in this figure that the velocity domain, in which the two critical levels can exist in addition to the normal level, is much larger than the upper domain in which only the normal level exists. A similar situation holds for larger-diameter pipes, since the stratified-to-intermittent

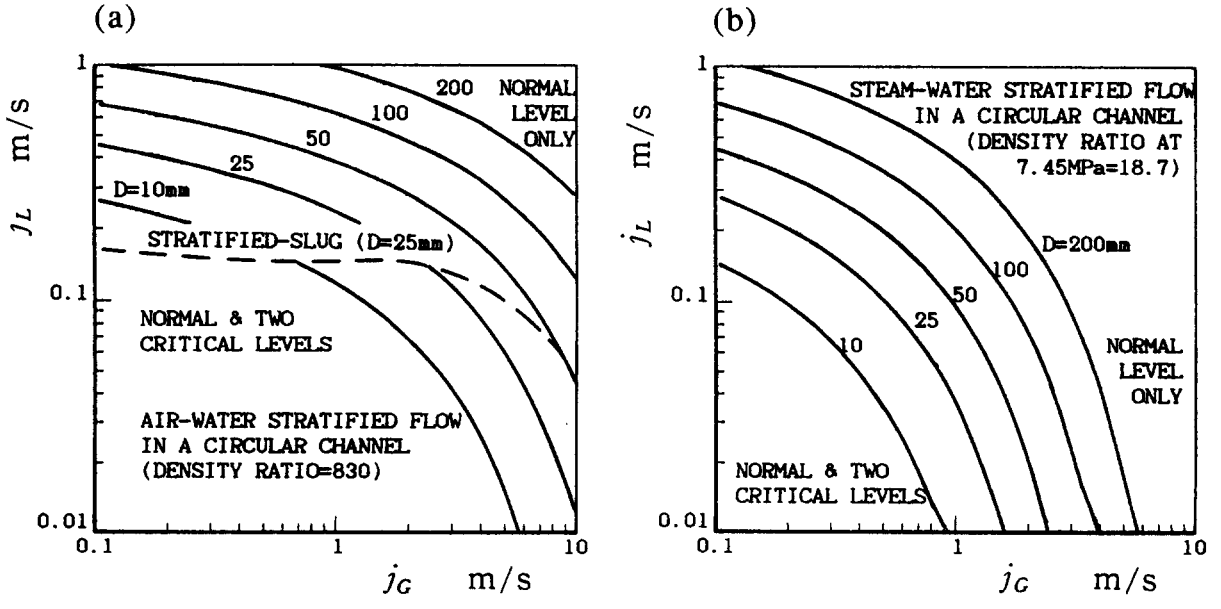

Figure 4. Velocity domain boundaries for critical liquid level existence.

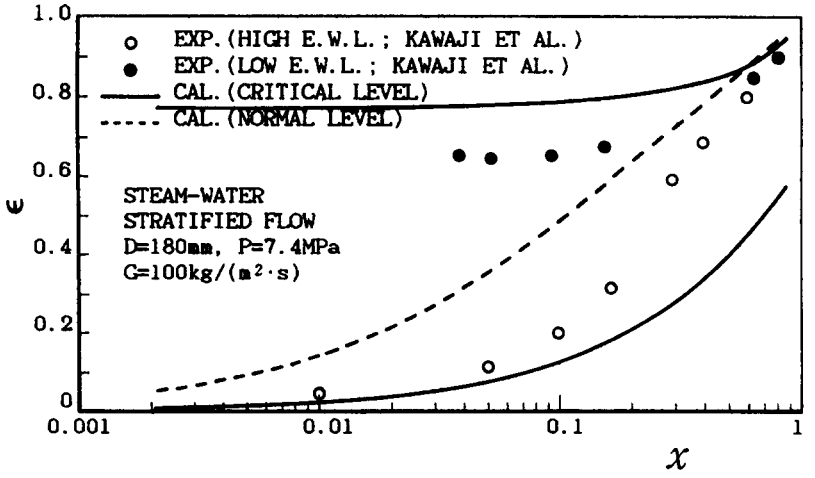

Figure 5. Comparison of model predictions of void fraction with Kawaji *et al.*'s (1987) data.

flow transition curve moves to higher superficial liquid velocities as the diameter is increased (Taitel & Dukler 1976b; Simpson *et al.* 1981; Nakamura *et al.* 1991).

Kawaji *et al.* (1987) performed steam–water stratified flow experiments in a 180 mm dia pipe and found that at high mass fluxes [$G = 1000$ and 400 kg/m^2 s, corresponding to $j_L = 1.1$ to 1.4 and 0.33 to 0.57 m/s, respectively, in figure 4(b)], the void fractions in the pipe were not influenced by the liquid discharge conditions at the exit of the pipe and the data matched those obtained for well-developed stratified flow. Figure 4(b) shows that at those superficial liquid velocities, there is only the normal liquid level possible regardless of the discharge conditions, which is consistent with the experimental findings.

On the other hand, at low mass velocities, two critical liquid levels are possible over a wide range of superficial gas velocities and therefore the void fraction is expected to vary along the flow direction, depending on the discharge condition at the exit. Figure 5 shows the average void fraction in the pipe, obtained from Kawaji *et al.*'s (1987) measurements at 1.36 and 6.94 m from the pipe exit, for different flow qualities at a fixed mass velocity of 100 kg/m^{2}s. Also shown are the void fractions predicted by [15] corresponding to the two critical liquid levels (solid lines) and the values predicted by [14] for zero-ILG (broken line). The experimental data obtained for the case of low exit water level [figure 6(a)] are given by solid symbols (●) and those for the case of high exit water level [figure 6(b)] by open symbols (○). The high exit water level data (○) are seen to lie between the zero-ILG predictions (broken line) and the lower solid line corresponding to the higher of the two critical levels predicted. On the other hand, the low exit water level data (●) lie mostly between

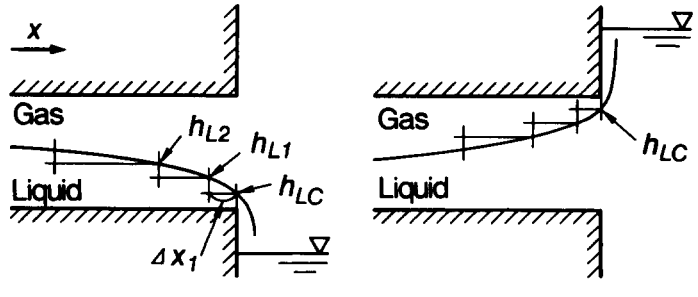

(a) Low exit water level ($dh_L/dx<0$)

(b) High exit water level ($dh_L/dx>0$)

Figure 6. Fluid discharge conditions and axial void calculation scheme.

the zero-ILG curve and the upper solid curve corresponding to the lower critical level. Similar results were obtained for the case of $G = 40\ \mathrm{kg/m^2\,s}$.

From these results, at low mass velocities, different liquid levels will be obtained depending on the liquid level in the discharge tank and, furthermore, the liquid level in the pipe is expected to vary gradually in the upstream direction, approaching the normal liquid level expected for a well-developed flow in a sufficiently long channel. Therefore, whether or not [15] has a solution is an important factor in the prediction of void fraction in stratified flow.

3.4. Calculation of the axial variation in the liquid level

When [15] has a solution and the channel exit conditions are as shown in figures 6(a) and 6(b), a method to calculate the axial variation of the liquid level in the flow direction is next described.

First, the two critical liquid levels are determined from [15], as discussed previously for specific gas and liquid flow rates. If the exit condition is as shown in figure 6(a) (low exit water level), the lower critical liquid level is selected as the boundary condition at the exit of the pipe. Although

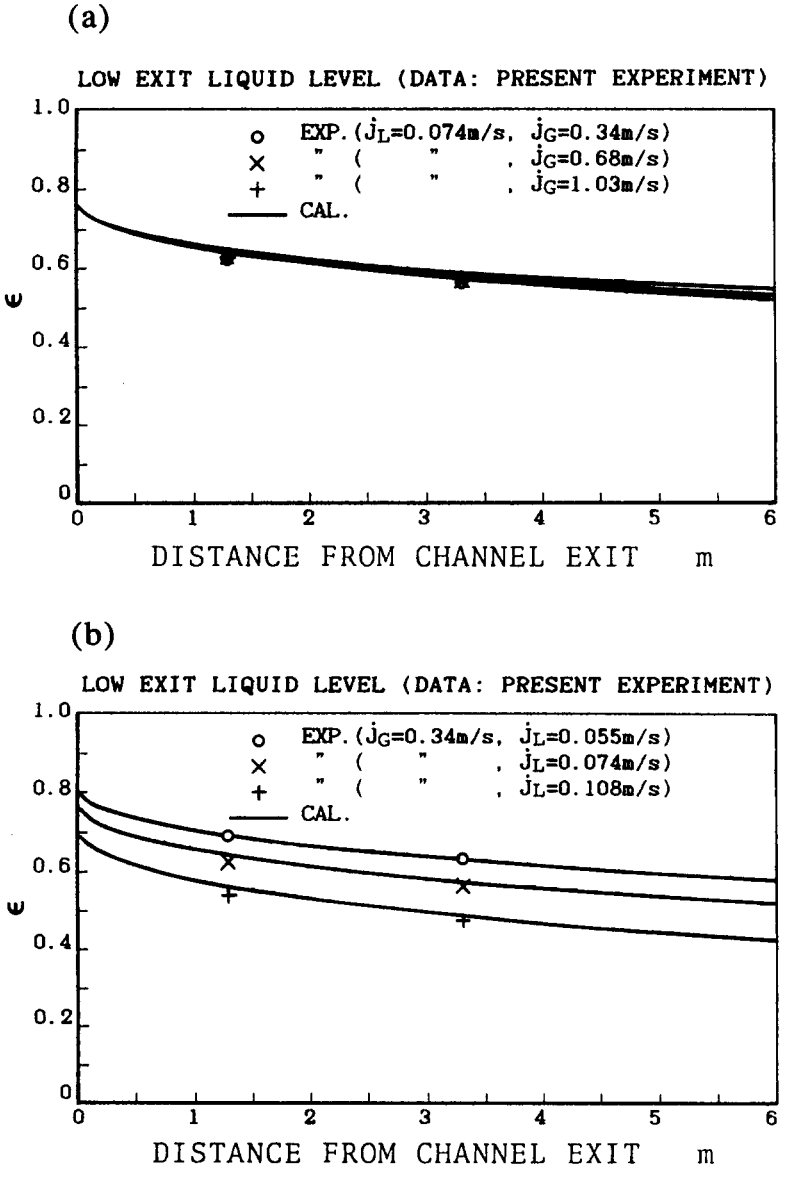

Figure 7. Comparison of model predictions with air–kerosene data (rectangular duct).

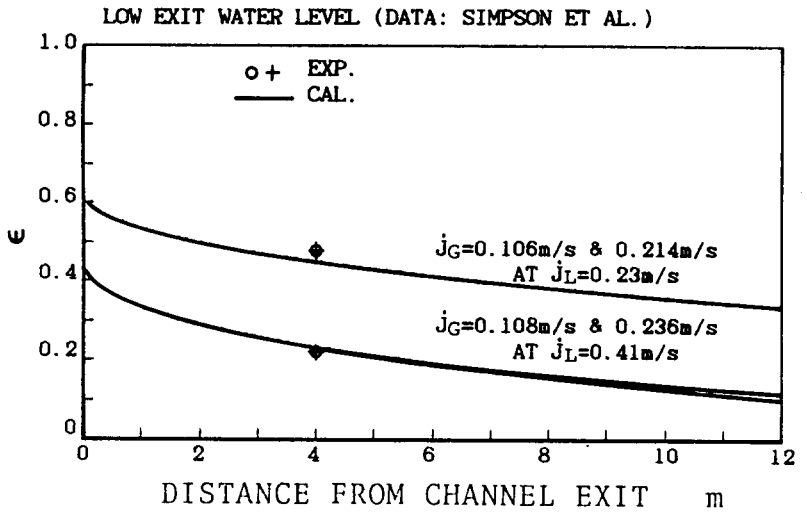

Figure 8. Comparison of model predictions with Simpson *et al.*'s (1981) air–water data (127 mm i.d. pipe).

Smith (1962) states that for an open-channel flow, the critical level will occur at a location slightly upstream of the pipe exit (by a length of up to about twice the critical level), and the actual liquid level at the exit is lower than the critical level, we assume that the critical liquid level is reached at the channel exit in order to simplify the calculations. On the other hand, for the case of high exit water level as shown in figure 6(b), the higher critical level is selected as the boundary condition at the pipe exit.

Next, we calculate the upstream liquid level step by step, by first selecting a certain incremental change in the liquid level and then solving [14] for the length increment Δx, as is done in open-channel flow calculations (French 1985). This procedure is effective in reducing the numerical error. In solving [14], the phasic velocities and area fractions, A_L and A_G, are the average values over the length increment Δx.

4. DISCUSSION

4.1. Comparison with the present experiments

In the present experiments, the liquid level in the outlet tank was always kept well below the rectangular channel exit, so the void fractions measured at two locations are compared with the predictions obtained with the lower critical liquid level as described in the previous section. Sample comparisons are shown in figures 7(a) and 7(b), in which the void fraction, ϵ, is plotted against the distance from the channel exit.

Figure 7(a) is for the case of a constant liquid flow rate with varying gas flow rates and both the predictions and the data show little difference among the three runs with different j_G. Figure 7(b) shows the constant gas flow rate case and the void fractions decrease as the superficial liquid velocity is increased, as expected. In all cases, the gas–liquid interface was smooth and the predictions clearly show the decreasing void fraction (or increasing liquid level) behavior in the upstream direction. The predictions are both qualitatively and quantitatively in excellent agreement with the measurement results.

4.2. Comparison with Simpson et al.'s (1981) data

Simpson *et al.* (1981) conducted horizontal air–water two-phase flow experiments in a 16 m long, 127 mm i.d. circular pipe and measured void fraction using a γ-densitometer. Some of their void fraction data from the stratified flow runs with a smooth interface are plotted in figure 8 along with the present model predictions for superficial liquid velocities of 0.23 and 0.40 m/s with varying gas flow rates. The effect of gas flow rate on void fraction is again insignificant and the model predicts the data very well.

4.3. Comparison with Kawaji et al.'s (1987) data

Some of the low mass flux void fraction data obtained by Kawaji *et al.* (1987) for steam-water stratified flows at a pressure of 7.5 MPa are compared with the present model in figures 9(a) and 9(b). Figure 9(a) is for the case of a low exit water level and shows the data for $G = 115$ (two runs with different flow qualities) and 42.8 kg/m^{2}s. In a steam–water system, the void fraction is again strongly dependent on mass velocity rather than quality and the present model predicts the data quite well.

Figure 9(b) shows the case of a high exit water level and the data are for the same mass velocity but at different qualities ($x = 0.050$ and 0.098). The interface was smooth in both runs and the model predictions are again in good agreement with the data. A drastic effect of the exit water level on the void fraction is clearly evident from a comparison of the two runs with about the same mass flux ($G = 103$ and 115 kg/m^2 s) and quality ($x = 0.093$ and 0.098), shown in figures 9(a) and 9(b). The void fraction increases from about 20 to 65% as the exit water level is changed from a level below the pipe to about 0.4 m above the pipe. The present model is seen to predict the effect of the exit water level extremely well.

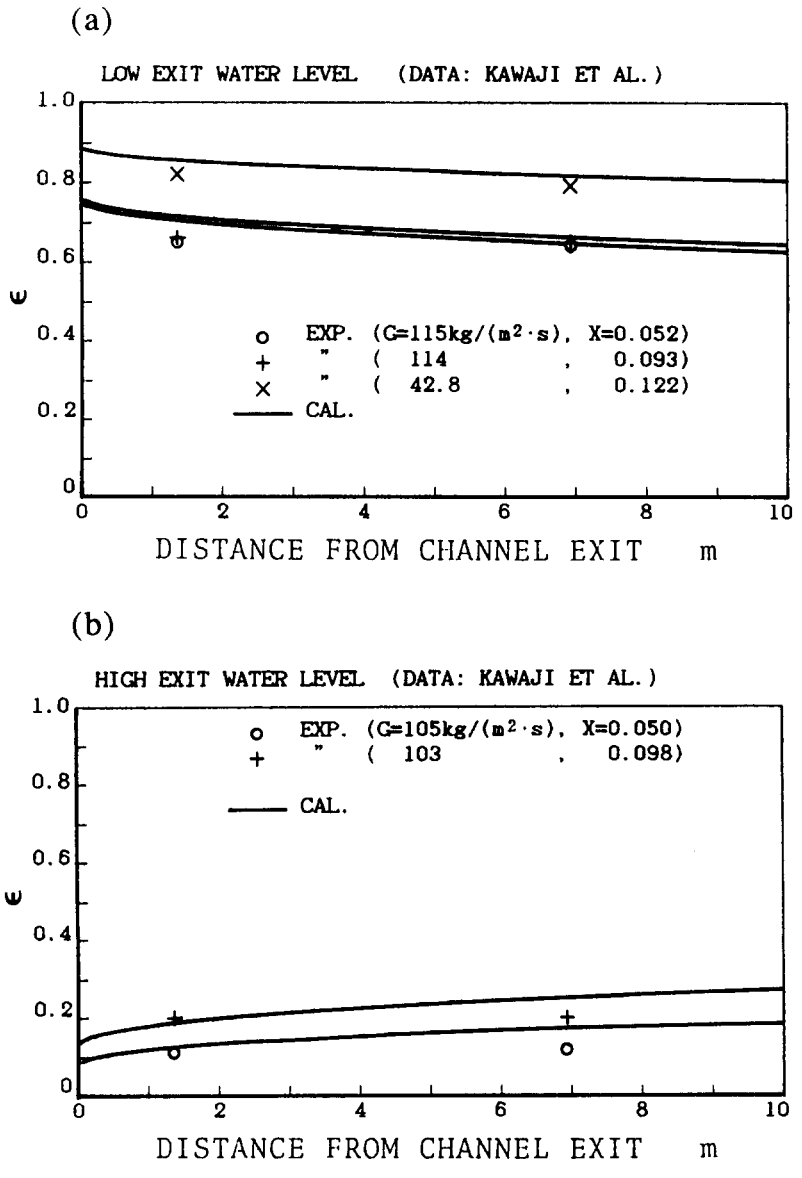

Figure 9. Comparison of model predictions with Kawaji *et al.*'s (1987) steam–water data (180 mm i.d. pipe, $P = 7.45$ MPa).

5. CONCLUSIONS

A one-dimensional momentum equation has been derived based on a two-fluid model and incorporating the ILG effect to predict the void fraction distribution in stratified two-phase flows in horizontal channels. An equation for determining the critical liquid level reached near the exit of the channel in stratified flow was also obtained. When there is no solution to the critical liquid level equation, the normal liquid level appearing in well-developed stratified flow without any ILG is attained. It was also shown that for a certain range of liquid and gas flow rates there are two solutions to the critical liquid level equation, corresponding to the two critical liquid levels that can be reached depending on the liquid discharge condition at the channel exit. A method was proposed to calculate the liquid level distribution in the channel using the critical liquid level at the channel exit as one of the boundary conditions. The model predictions were compared with the void fraction data obtained in a rectangular channel in this work and in large-diameter pipes previously reported by Simpson *et al.* (1981) and Kawaji *et al.* (1987). Excellent agreement was shown for all cases with a smooth interface.

Acknowledgements—This work was supported by the Natural Sciences and Engineering Research Council of Canada, through an operating grant to M. Kawaji and an International Fellowship to M. Sadatomi.

REFERENCES

BISHOP, A. A. & DESHPANDE, S. D. 1986 Interfacial level gradient effects in horizontal Newtonian liquid–gas stratified flow—I. *Int. J. Multiphase Flow* **12,** 957–975.

BROWN, R. C. ANDREUSSI, P. & ZANELLI, S. 1978 The use of wire probes for the measurement of liquid film thickness in annular gas–liquid flows. *Can. J. Chem. Engng* **56,** 754–757.

FRENCH, R. H. 1985 *Open-channel Hydraulics*. McGraw-Hill, New York.

KAWAJI, M., ANODA, Y., NAKAMURA, H. & TASAKA, T. 1987 Phase and velocity distributions and holdup in high-pressure steam/water stratified flow in a large diameter horizontal pipe. *Int. J. Multiphase Flow* **13,** 145–159.

KOIZUMI, Y., YAMAMOTO, N. & TASAKA, K. 1990 Air/water two-phase flow in a horizontal large-diameter pipe (1st Report, flow regime). *Trans. JSME* **56B,** 3745–3749.

KOSKIE, J. E., MUDAWAR, I. & TIEDERMAN, W. G. 1989 Parallel-wire probes for measurement of thick liquid films. *Int. J. Multiphase Flow* **15,** 521–530.

LORENCEZ, C., CHANG, T. & KAWAJI, M. 1991 Investigation of turbulent momentum transfer at a gas–liquid interface in a horizontal countercurrent stratified flow. *ASME FED* **110,** 97–102.

NAKAMURA, H., ANODA, Y. & KUKITA, Y. 1991 Flow regime transitions in high-pessure steam–water horizontal pipe two-phase flow. In *ANS Proc. 1991 National Heat Transfer Conf.*, Vol. 5, pp. 269–276.

SADATOMI, M., SATO, Y. & SARUWATARI, S. 1982 Two-phase flow in vertical noncircular channels. *Int. J. Multiphase Flow* **8,** 641–655.

SHAH, R. H. & LONDON, A. L. 1978 *Laminar Flow Forced Convection in Ducts*, pp. 276–279. Academic Press, New York.

SIMPSON, H. C. ROONEY, D. H. & GRATTAN, E. 1981 Two-phase flow studies in large diameter horizontal tubes. NEL Report No. 667.

SMITH, C. D. 1962 Brink depth for a circular channel. *Proc. Am. Soc. Civ. Engrs J. Hydraul. Div.* **HY-88,** 125–134.

TAITEL, Y. & DUKLER, A. E. 1976a A theoretical approach to the Lockhart–Martinelli correlation for stratified flow. *Int. J. Multiphase Flow* **2,** 591–595.

TAITEL, Y. & DUKLER, A. E. 1976b A model for predicting flow regime transitions in horizontal and near horizontal gas–liquid flow. *AIChE Jl* **22,** 47–55.

TAITEL, Y. & DUKLER, A. E. 1987 Effect of pipe length on the transition boundaries for high-viscosity liquids. *Int. J. Multiphase Flow* **13,** 577–581.